Gulf Journal of Mathematics
Vol 24, Issue 2 (2026) 1-18

ISSN: 2309-4966
https://doi.org/10.56947/08bmn821

FRACTIONAL TUBERCULOSIS DYNAMICS AND OPTIMAL CONTROL

DESIRE OUEDRAOGO[1*], HAMADOUM DICKO[2] and ADAMA KIEMTORE[3]

Abstract. We develop a fractional-order model to investigate tuberculosis transmission and control strategies. The fractional formulation accounts for memory effects and long-term dependence relevant to chronic infectious diseases. The basic reproduction number is derived using the next-generation matrix method. We establish the existence, positivity, and boundedness of solutions and investigate the global stability of the disease-free and the endemic equilibria. Sensitivity analysis identifies the parameters with the greatest influence on disease transmission. An optimal control problem incorporating prevention and treatment reinforcement is formulated and analyzed. Numerical simulations support the theoretical findings.

Keywords. Tuberculosis model; Caputo derivative; Basic reproduction number; Global stability; Optimal control; Numerical simulation.
2020 Mathematics Subject Classification. 26A33, 34A08, 49K15, 92C60, 93C15.

1. Introduction

Despite considerable progress in diagnosis, treatment, and prevention programs, tuberculosis continues to cause significant morbidity and mortality, particularly in developing countries where access to healthcare remains limited. According to the World Health Organization (WHO) [23], tuberculosis is among the leading causes of death from a single infectious agent, with millions of new infections reported annually. The persistence of latent infection, the long incubation period, treatment failure, relapse, and the emergence of drug-resistant strains make tuberculosis control particularly challenging. These difficulties highlight the necessity of developing effective prevention and treatment strategies supported by rigorous scientific analysis.

Several mathematical studies have been devoted to tuberculosis dynamics. Zhang et al. [25] proposed a mathematical model based on tuberculosis transmission data in China. Yang et al. [24] studied a tuberculosis model with vaccination and treatment and investigated its global stability and optimal control properties.

Date: Received: Aug 26, 2026; Revised: Sep 23, 2026; Accepted: Oct 1, 2026.
* Corresponding author
© The Author(s) 2026. This article is licensed under a Creative Commons Attribution-NonCommercial-NoDerivatives 4.0 International License. To view a copy of the licence, visit https://creativecommons.org/licenses/by-nc-nd/4.0/.

In [7], Dicko and Traoré also investigated the impact of hospital resources on tuberculosis transmission through a mathematical model, highlighting the essential role of healthcare capacity in reducing disease prevalence and improving disease management policies. Li et al. [17] performed a global stability and optimal control analysis using tuberculosis case data from the United States.

These studies have significantly improved the understanding of tuberculosis transmission and have shown the importance of treatment, vaccination, and early intervention strategies. However, most classical models are formulated using ordinary differential equations of integer order, which may not fully capture the memory effects and hereditary characteristics frequently observed in chronic infectious diseases such as tuberculosis. Since TB involves latency, delayed progression, and possible reactivation, its transmission dynamics are strongly influenced by past disease history, making fractional-order modeling particularly relevant.

Several works have demonstrated the effectiveness of fractional derivatives in modeling infectious diseases. Kilicman et al. [13] studied a fractional-order dengue model and showed the importance of fractional derivatives in describing epidemic evolution. Traoré et al. [21] studied a fractional-order model of a vector-borne disease and developed a comprehensive qualitative analysis together with an optimal control problem to evaluate the effectiveness of intervention strategies. Balzotti et al. Balzotti et al. [2] analyzed a fractional SIS model and highlighted the role of fractional dynamics in describing epidemic persistence and decline. More recently, Daimary and Paul [5] investigated a fractional-order mathematical model using Caputo-type derivatives and established existence, boundedness, and stability results together with sensitivity analysis. In the epidemiological context, Chagdal et al. [4] studied a fractional multi-strain epidemic model and derived conditions for the local and global stability of disease-free and endemic equilibria. These recent contributions further demonstrate the relevance of fractional-order approaches for capturing memory effects and analyzing the stability of complex dynamical systems.

Concerning tuberculosis specifically, several recent studies have emphasized the usefulness of Caputo fractional derivatives. Bhatter et al. [3] introduced a Caputo fractional model for tuberculosis and showed that fractional-order formulations improve model accuracy significantly compared to integer-order systems. Dicko et al. [8] proposed a fractional-order tuberculosis model and analyzed its dynamical properties, including the existence of solutions, the stability of equilibria, and the application of optimal control to reduce disease transmission. Khan et al. [12] investigated the behavior of a fractional tuberculosis system under different epidemiological conditions.

Although these contributions confirm the importance of fractional-order models in tuberculosis research, many of them mainly focus on theoretical analysis and numerical simulations without incorporating optimal prevention and treatment strategies into the modeling framework. Since effective tuberculosis management requires both reducing disease transmission and improving treatment outcomes, it is relevant to use optimal control theory to determine cost-effective intervention policies.

The rest of this paper is organized as follows: Section 2 defines the model; Section 3 derives the basic reproduction number and analyzes the global stability of the disease-free equilibrium; Section 4 addresses the existence, uniqueness, and global stability of the endemic equilibrium; Section 5 presents a sensitivity analysis; Section 6 formulates and analyzes the optimal control problem; Section 7 simulates various epidemic scenarios; and Section 8 concludes and discusses perspectives.

2. Model description

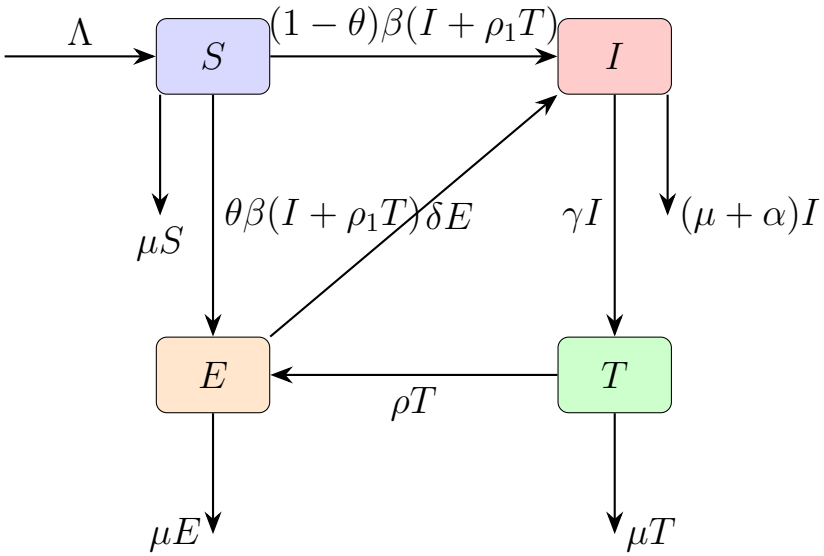


Figure 1. Flow diagram of the model

We consider a population with a constant recruitment rate Λ, and a death rate μ. Due to the tuberculosis, the population is subdivided into four epidemiological classes. The class S of susceptible individuals, the class E of individuals infected with tuberculosis in the latent stage, the class I of individuals infected with active tuberculosis, and the class T of individuals under treatment. Let $S(t), E(t), I(t), T(t)$ be the sizes of the respective classes at time $t \geq 0$. The total population size denoted by $N(t)$ is given by $N(t) = S(t) + E(t) + I(t) + T(t)$.
All new individuals enter the susceptible class S at a constant recruitment rate Λ. Susceptible individuals are exposed to tuberculosis through effective contact with infectious individuals in the active stage I, as well as with treated individuals, who may still contribute to transmission at a reduced level. The modification parameter ρ_1 measures the relative infectiousness of treated individuals compared to actively infectious individuals, where $0 \leq \rho_1 \leq 1$. Consequently, the force of infection is expressed by $\beta\big(I + \rho_1 T\big)$, where β denotes the effective transmission rate.
After infection, a proportion θ of newly infected susceptible individuals enters the latent tuberculosis class E, while the remaining proportion $1 - \theta$ progresses directly to the active infectious class I. Individuals in the latent stage are infected but not infectious. They may develop active tuberculosis at a progression rate δ.

Individuals in the active infectious class receive treatment at a constant rate γ and move to the treatment compartment T. Treated individuals may recover partially and return to the latent class at a rate ρ, reflecting incomplete bacterial clearance or persistence of latent infection after treatment.
Natural mortality, due to causes unrelated to tuberculosis, affects all individuals at a constant rate μ. In addition, individuals in the active infectious class experience disease-induced mortality at a rate α.
Taking into account all the above assumptions and epidemiological transitions, the dynamics of the tuberculosis model is governed by the diagram given in Fig.1.
The system of differential equations of the model is:

$$\begin{cases} \dfrac{dS}{dt} = \Lambda - \beta S(I + \rho_1 T) - \mu S, \\ \dfrac{dE}{dt} = \theta\beta S(I + \rho_1 T) - (\mu + \delta)E + \rho T, \\ \dfrac{dI}{dt} = (1-\theta)\beta S(I + \rho_1 T) + \delta E - (\mu + \alpha + \gamma)I, \\ \dfrac{dT}{dt} = \gamma I - (\mu + \rho)T, \\ S(0) \geq 0, \quad E(0) \geq 0, \quad I(0) \geq 0, \quad T(0) \geq 0. \end{cases} \tag{2.1}$$

This model is based on a classical framework of ordinary differential equations. It does not take into account the memory effect, which is an essential element in epidemiological dynamics.
To incorporate the memory effect, we reformulate the model (2.1) using the Caputo operator, denoted by ${}^{C}D_t^q$. We get then, the fractional-order model :

$$\begin{cases} {}^{C}D_t^q S = \Lambda - \beta S(I + \rho_1 T) - \mu S, \\ {}^{C}D_t^q E = \theta\beta S(I + \rho_1 T) - (\mu + \delta)E + \rho T, \\ {}^{C}D_t^q I = (1-\theta)\beta S(I + \rho_1 T) + \delta E - (\mu + \alpha + \gamma)I, \\ {}^{C}D_t^q T = \gamma I - (\mu + \rho)T, \\ S(0) \geq 0, \quad E(0) \geq 0, \quad I(0) \geq 0, \quad T(0) \geq 0. \end{cases} \tag{2.2}$$

Let consider the feasible region $\mathcal{D}$ defined by

$$\mathcal{D} = \left\{ (S, E, I, T) \in \mathbb{R}_+^4 : \ S + E + I + T \leq \frac{\Lambda}{\mu} \right\}. \tag{2.3}$$

Proposition 2.1. *The domain $\mathcal{D}$ is positively invariant for system (2.2).*

Proof. We examine the direction of the vector field on each boundary hyperplane of $\mathbb{R}^4_+$.

$$\begin{aligned}
{}^{C}D_t^q S(t)\big|_{\{S=0,\ E\geq 0,\ I\geq 0,\ T\geq 0\}} &= \Lambda \geq 0,\\
{}^{C}D_t^q E(t)\big|_{\{E=0,\ S\geq 0,\ I\geq 0,\ T\geq 0\}} &= \theta\beta S(I+\rho_1 T)+\rho T \geq 0,\\
{}^{C}D_t^q I(t)\big|_{\{I=0,\ S\geq 0,\ E\geq 0,\ T\geq 0\}} &= (1-\theta)\beta\rho_1 ST+\delta E \geq 0,\\
{}^{C}D_t^q T(t)\big|_{\{T=0,\ S\geq 0,\ E\geq 0,\ I\geq 0\}} &= \gamma I \geq 0.
\end{aligned} \tag{2.4}$$

Hence, the vector field points inward on every boundary of $\mathbb{R}^4_+$. By the standard positivity result for Caputo fractional systems [9, 19], every solution starting in $\mathbb{R}^4_+$ remains in $\mathbb{R}^4_+$ for all $t \geq 0$. Therefore, all state variables remain nonnegative. Using the classical inverse Laplace transforms involving Mittag–Leffler functions [20, 1], whenever $N(0) \leq \frac{\Lambda}{\mu}$. Hence every trajectory starting in $\mathcal{D}$ remains in $\mathcal{D}$, which proves that $\mathcal{D}$ is positively invariant.

□

3. Disease-free state stability

In this section, we establish the existence of the disease-free equilibrium of system (2.2) and derive the associated stability results. We also compute the basic reproduction number.

The disease-free equilibrium corresponds to the absence of tuberculosis infection in the population, that is, $E = 0, \quad I = 0, \quad T = 0.$

Therefore, the model (2.2) admits the unique disease-free equilibrium

$$\mathcal{E}_0 = \left(\frac{\Lambda}{\mu},\ 0,\ 0,\ 0\right). \tag{3.1}$$

Using the next-generation matrix method of van den Driessche and Watmough[22], the basic reproduction number of system (2.2) is obtained as

$$\mathcal{R}_0 = \rho(FV^{-1}) = \frac{\Lambda\beta\left[\delta+(1-\theta)\mu\right](\gamma\rho_1+\mu+\rho)}{\mu\left[(\mu+\delta)(\mu+\rho)(\mu+\alpha)+(\mu+\delta+\rho)\mu\gamma\right]}.$$

The local stability result of the disease-free equilibrium $\mathcal{E}_0$ is stated as follows.

Theorem 3.1. *The disease-free equilibrium $\mathcal{E}_0$ of system (2.2), is globally asymptotically stable in the feasible region $\mathcal{D}$ whenever $\mathcal{R}_0 \leq 1$.*

Proof. To establish the global asymptotic stability of the disease-free equilibrium, we consider the following Lyapunov function

$$H(S,E,I,T) = \delta E + (\mu+\delta)I + AT,$$

where the positive constant A is chosen as

$$A = \frac{\rho_1\beta\delta S_0 + \delta\rho + \rho_1\beta(1-\theta)(\mu+\delta)S_0}{\mu+\rho}.$$

Clearly, $H(S,E,I,T) \geq 0$ for all $(S,E,I,T) \in \Omega$, and $H(S,E,I,T) = 0$ if and only if $E = I = T = 0$.

Now, taking the Caputo fractional derivative of H along the solutions of system (2.2), we obtain

$$ {}^{C}D_t^q H(S,E,I,T) = \delta\, {}^{C}D_t^q L + (\mu+\delta)\, {}^{C}D_t^q I + A\, {}^{C}D_t^q T. $$

Substituting the equations of system (2.2) then simplifying, since $S(t) \leq S_0 = \dfrac{\Lambda}{\mu}$ for all $t \geq 0$, and after straightforward algebraic manipulations, we obtain

$$ {}^{C}D_t^q H(S,E,I,T) \leq \frac{(\mu+\delta)(\mu+\rho)(\mu+\alpha)+(\mu+\delta+\rho)\mu\gamma}{\mu+\rho}(\mathcal{R}_0-1)I. $$

Hence, whenever $\mathcal{R}_0 \leq 1$, we have ${}^{C}D_t^q H(S,E,I,T) \leq 0$. Moreover, ${}^{C}D_t^q H(S,E,I,T) = 0$ if and only if $(S(t),E(t),I(t),T(t)) = (\frac{\Lambda}{\mu},0,0,0) \quad \text{as} \quad t \to \infty$. Hence, the largest compact invariant set contained in $\left\{(S,L,I,T)\in\mathcal{D} \;\middle|\; {}^{C}D_t^q H(S,E,I,T)=0\right\}$ is reduced to the singleton $\{\mathcal{E}_0\}$. Therefore, by the fractional LaSalle invariance principle (see [15]), every solution of system (2.2) with initial conditions in $\mathcal{D}$ approaches the disease-free equilibrium $\mathcal{E}_0$ as $t \to \infty$, provided that $\mathcal{R}_0 \leq 1$. Thus, the disease-free equilibrium $\mathcal{E}_0$ is globally asymptotically stable in $\mathcal{D}$, when $\mathcal{R}_0 \leq 1$. □

4. Existence and stability of endemic equilibrium

Now we show existence and uniqueness of an endemic equilibrium, and establish its global stability in $\mathcal{D}$, whenever $\mathcal{R}_0 > 1$.

4.1. Existence and uniqueness of the endemic equilibrium.

In this subsection we show that whenever $\mathcal{R}_0 > 1$, System (2.2) admits an unique endemic equilibrium.

Proposition 4.1. *System (2.2) admits a unique endemic equilibrium whenever $\mathcal{R}_0 > 1$, and has no endemic equilibrium whenever $\mathcal{R}_0 \leq 1$.*

Proof. We denote by $\mathcal{E}^* = (S^*, E^*, I^*, T^*)$ the endemic equilibrium of system (2.2), where all components are strictly positive. At equilibrium,

$$ {}^{C}D_t^q S = {}^{C}D_t^q E = {}^{C}D_t^q I = {}^{C}D_t^q T = 0. $$

Hence, $\mathcal{E}^*$ satisfies the algebraic system

$$ \begin{cases} \Lambda - \beta S^*(I^* + \rho_1 T^*) - \mu S^* = 0, \\ \theta\beta S^*(I^* + \rho_1 T^*) - (\mu+\delta)E^* + \rho T^* = 0, \\ (1-\theta)\beta S^*(I^* + \rho_1 T^*) + \delta E^* - (\mu+\alpha+\gamma)I^* = 0, \\ \gamma I^* - (\mu+\rho)T^* = 0. \end{cases} \tag{4.1} $$

We first derive explicit expressions for S^*, E^* and T^* in terms of I^*.
From the fourth equation of (4.1), we obtain by setting: $a_1 = \dfrac{\beta(\mu+\rho+\rho_1\gamma)}{\mu+\rho}$

$$ S^* = \frac{\Lambda}{\mu + a_1 I^*}, E^* = \frac{\theta a_1 S^* I^* + \rho T^*}{\mu+\delta}, I^* = \frac{\mu}{a_1}\left(\mathcal{R}_0 - 1\right), T^* = \frac{\gamma}{\mu+\rho} I^*. \tag{4.2} $$

Therefore:

- If $\mathcal{R}_0 > 1$, then $I^* > 0$, and consequently $S^* > 0$, $E^* > 0$, and $T^* > 0$. Hence the model admits a unique endemic equilibrium $\mathcal{E}^*$,
- If $\mathcal{R}_0 \leq 1$, then $I^* \leq 0$, which is biologically meaningless. Thus, no endemic equilibrium exists in this case.

□

4.2. **Stability of the endemic equilibrium for the fractional model.** Now, we establish the global asymptotic stability of the endemic equilibrium $\mathcal{E}^*$ of System (2.2), in $\mathcal{D} \setminus \{E = I = T = 0\}$, whenever $\mathcal{R}_0 > 1$.

Theorem 4.2. *The endemic equilibrium $\mathcal{E}^* = (S^*, E^*, I^*, T^*)$ of System (2.2), is globally asymptotically stable in $\mathcal{D} \setminus \{E = I = T = 0\}$, if $\mathcal{R}_0 > 1$.*

Proof. For $\mathcal{R}_0 > 1$, the endemic equilibrium $\mathcal{E}^* = (S^*, E^*, I^*, T^*)$ satisfies

$$\begin{aligned} \Lambda &= \beta S^* \left(I^* + \rho_1 T^*\right) + \mu S^*, \\ (\mu + \delta) E^* &= \theta \beta S^* \left(I^* + \rho_1 T^*\right) + \rho T^*, \\ (\mu + \alpha + \gamma) I^* &= (1 - \theta) \beta S^* \left(I^* + \rho_1 T^*\right) + \delta E^*, \\ (\mu + \rho) T^* &= \gamma I^*. \end{aligned} \tag{4.3}$$

To establish the global stability of $\mathcal{E}^*$, we consider the Volterra-type Lyapunov function

$$\begin{aligned} G = &\left(S - S^* - S^* \ln \frac{S}{S^*}\right) + B_1 \left(E - E^* - E^* \ln \frac{E}{E^*}\right) \\ &+ B_2 \left(I - I^* - I^* \ln \frac{I}{I^*}\right) + B_3 \left(T - T^* - T^* \ln \frac{T}{T^*}\right), \end{aligned}$$

where $B_1,\ B_2,\ B_3 > 0$ are constants to be determined.
Clearly, $G \geq 0$, and

$$G = 0 \quad \Longleftrightarrow \quad (S, E, I, T) = (S^*, E^*, I^*, T^*).$$

Using the fractional derivative property for convex Lyapunov functions, we obtain

$$\begin{aligned} {}^C D_t^q G = &\left(1 - \frac{S^*}{S}\right) {}^C D_t^q S + B_1 \left(1 - \frac{E^*}{E}\right) {}^C D_t^q E \\ &+ B_2 \left(1 - \frac{I^*}{I}\right) {}^C D_t^q I + B_3 \left(1 - \frac{T^*}{T}\right) {}^C D_t^q T. \end{aligned}$$

Substituting system (2.2) and using (4.3), we get :

$$\begin{aligned} {}^C D_t^q G = &- \mu \frac{(S - S^*)^2}{S} + \beta S^* I^* \left(1 - \frac{S^*}{S}\right) + \rho_1 \beta S^* T^* \left(1 - \frac{S^*}{S}\right) \\ &+ \beta S (I + \rho_1 T) \left[B_1 \theta + B_2 (1 - \theta) - 1\right] + I \left[\beta S^* - B_2 (\mu + \alpha + \gamma) + B_3 \gamma\right] \\ &+ T \left[\rho_1 \beta S^* + B_1 \rho - B_3 (\mu + \rho)\right] + E \left[B_2 \delta - B_1 (\mu + \delta)\right] - S B_2 (1 - \theta) \beta I^* \\ &- \frac{SI}{E} B_1 \theta \beta E^* - \frac{ST}{E} B_1 \theta \rho_1 \beta E^* - \frac{T}{E} B_1 \rho E^* - \frac{ST}{I} B_2 (1 - \theta) \rho_1 \beta I^* \\ &- \frac{E}{I} B_2 \delta I^* - \frac{I}{T} \gamma B_3 T^* + B_1 \theta \beta S^* (I^* + \rho_1 T^*) + B_1 \rho T^* \\ &+ B_2 (1 - \theta) \beta S^* (I^* + \rho_1 T^*) + B_2 \delta E^* + B_3 \gamma I^*, \end{aligned}$$

such as

$$B_1 = \frac{\delta}{\mu+\delta}B_2, \quad B_2 = \frac{\mu+\delta}{(1-\theta)(\mu+\delta)+\theta\delta}, \quad \text{and} \quad B_3 = \frac{\rho B_1 + \rho_1(\mu+\alpha+\gamma)B_2}{\mu+\rho+\rho_1\gamma}.$$

For convenience, define $x = \frac{S}{S^*}$, $y = \frac{E}{E^*}$, $z = \frac{I}{I^*}$, $u = \frac{T}{T^*}$.
Then, after substitution, we obtain

$$\begin{aligned}
{}^{C}D_t^q G = &-\mu\frac{(S-S^*)^2}{S} + B_2(1-\theta)\beta S^* I^*\left(2-\frac{1}{x}-x\right)\\
&+ B_2(1-\theta)\rho_1\beta S^* T^*\left(2-\frac{1}{x}-\frac{xu}{z}\right) + B_1\theta\beta S^* I^*\left(2-\frac{1}{x}-\frac{xz}{y}\right)\\
&+ B_1\theta\rho_1\beta S^* T^*\left(2-\frac{1}{x}-\frac{xu}{y}\right) + B_1\rho T^*\left(1-\frac{u}{y}\right) + B_2\delta E^*\left(1-\frac{y}{z}\right)\\
&+ B_3\gamma I^*\left(1-\frac{z}{u}\right).
\end{aligned}$$

Proceeding exactly as in the classical case, using (4.3) and the arithmetic–geometric mean inequality ([11]), we obtain: ${}^{C}D_t^q G \leq 0$. Moreover, ${}^{C}D_t^q G = 0$ if and only if $S = S^*$ and $\frac{E}{E^*} = \frac{I}{I^*} = \frac{T}{T^*}$. Hence, by the fractional LaSalle invariance principle (see [15]), every solution approaches the largest invariant set contained in $\{\mathcal{E}^*\}=\{(S,E,I,T) \in \mathcal{D} : S = S^*; \frac{E}{E^*} = \frac{I}{I^*} = \frac{T}{T^*}\}$. It is effortless to show that $\{\mathcal{E}^*\}$, since $\mathcal{E}^*$ is the unique equilibrium of System (2.2). Thus, the only invariant set is the singleton $\{\mathcal{E}^*\}$. Consequently, the endemic equilibrium $\mathcal{E}^*$ is globally asymptotically stable in $\mathcal{D} \setminus \{E = I = T = 0\}$. □

5. Sensitivity Analysis

Sensitivity analysis is a fundamental mathematical tool used to identify the parameters that have the greatest influence on the transmission dynamics of an infectious disease. In particular, it helps determine which epidemiological and biological parameters should be targeted to reduce disease spread most effectively. In this work, the sensitivity analysis is performed with respect to the basic reproduction number $\mathcal{R}_0$.
Following [14, 18], the normalized forward sensitivity index of a parameter p, denoted by $C_p^{\mathcal{R}_0}$, is defined by

$$C_p^{\mathcal{R}_0} = \frac{\partial \mathcal{R}_0}{\partial p}\frac{p}{\mathcal{R}_0} = \frac{\partial \ln \mathcal{R}_0}{\partial \ln p}. \tag{5.1}$$

This quantity measures the relative change in $\mathcal{R}_0$ resulting from a relative change in the parameter p. Specifically, a relative variation of $i\%$ in p produces approximately a variation of $C_p^{\mathcal{R}_0} \times i\%$ in $\mathcal{R}_0$.
A positive sensitivity index indicates that increasing the parameter increases disease transmission, whereas a negative index indicates that increasing the parameter contributes to reduce disease spread.
It is important to note that $\mathcal{R}_0$ does not depend explicitly on the fractional order q, which means that the memory effect influences the transient dynamics of the disease but does not alter the epidemic threshold.

An examples of parameters sensitivities are displayed in Fig. 2. These results suggest that the most effective intervention strategies should focus on:

- reducing the transmission coefficient β through early detection, isolation, and prevention policies,
- increasing the treatment rate γ through rapid diagnosis and adherence to treatment,
- reducing the infectious contribution of treated individuals by minimizing ρ_1,
- improving control of progression from infection to active tuberculosis.

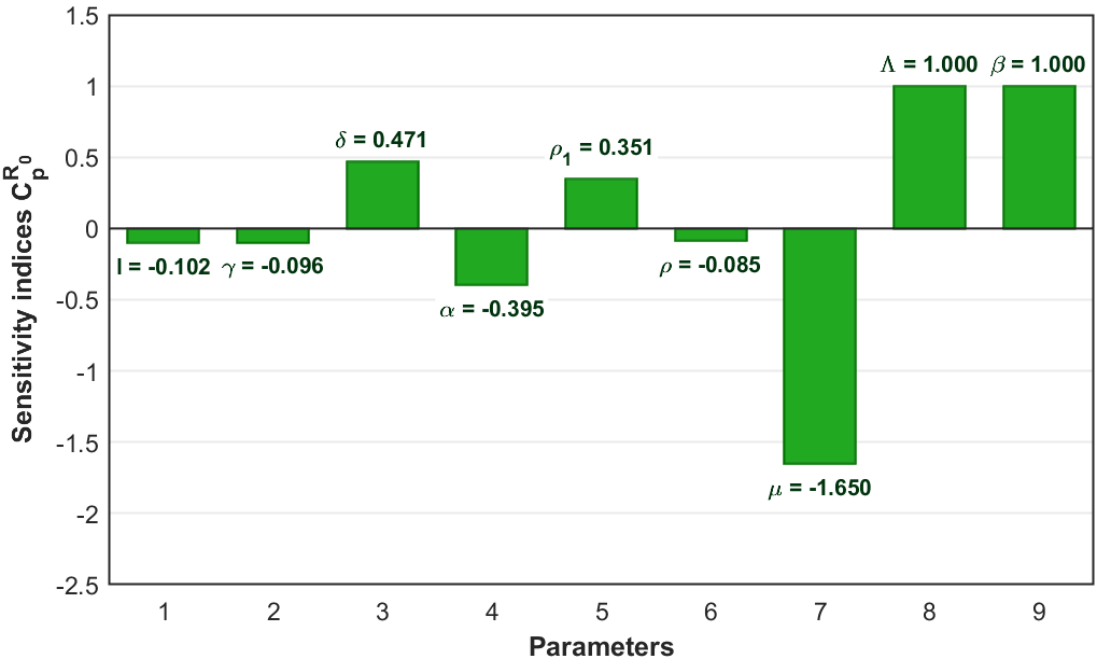


FIGURE 2. Sensitivity indices of $\mathcal{R}_0$. The parameters values used are $\Lambda = 100$, $\mu = 0.05$, $\beta = 0.00004$, $\rho_1 = 0.15$, $\theta = 0.75$, $\delta = 0.08$, $\alpha = 0.03$, $\gamma = 0.12$, $\rho = 0.02$.

Therefore, sensitivity analysis provides important quantitative guidance for designing optimal tuberculosis control strategies and supports the development of the optimal control framework presented in the next section.

6. Optimal Control

In this section we formulate and solve an optimal control problem associated with the controlled fractional tuberculosis model (2.2). The objective is to determine efficient prevention and treatment strategies that minimize the number of infectious individuals together with the implementation costs of the control measures over a fixed intervention period $[0, t_f]$.
We consider the following time-dependent controls:

- $u_1(t)$: prevention campaign reducing effective transmission,

- $u_2(t)$: treatment reinforcement increasing the recovery rate of infectious individuals.

These controls are assumed measurable and bounded such that

$$0 \leq u_1(t) \leq 1, \qquad 0 \leq u_2(t) \leq 1, \qquad t \in [0, t_f].$$

The controlled fractional system is given by

$$\begin{cases} {}^{C}D_t^q S = \Lambda - (1-u_1)\beta S(I + \rho_1 T) - \mu S, \\ {}^{C}D_t^q E = \theta(1-u_1)\beta S(I + \rho_1 T) - (\mu + \delta)E + \rho T, \\ {}^{C}D_t^q I = (1-\theta)(1-u_1)\beta S(I + \rho_1 T) + \delta E - (\mu + \alpha + \gamma + u_2)I, \\ {}^{C}D_t^q T = (\gamma + u_2)I - (\mu + \rho)T. \end{cases} \tag{6.1}$$

We seek to minimize the infectious burden and the cost of interventions through the objective functional

$$J(u_1, u_2) = \int_0^{t_f} \left(K_1 I(t) + K_2 T(t) + \frac{B_1}{2} u_1^2(t) + \frac{B_2}{2} u_2^2(t) \right) dt, \tag{6.2}$$

where:

- $K_1 > 0$ and $K_2 > 0$ represent the social and medical costs associated with infectious and treated individuals, respectively;
- $B_1 > 0$ and $B_2 > 0$ are weighting constants associated with the implementation costs of prevention and treatment reinforcement;
- t_f denotes the final time of the control horizon.

The admissible control set is defined by

$$\mathcal{U}_{ad} = \left\{ (u_1, u_2) \in L^{\infty}[0, t_f]^2 : 0 \leq u_1(t) \leq 1,\ 0 \leq u_1(t) \leq 1,\ t \in [0, t_f] \right\}. \tag{6.3}$$

According to Pontryagin's Maximum Principle, we define the Hamiltonian function by

$$\begin{aligned} \mathcal{H} = {} & K_1 I + K_2 T + \frac{B_1}{2} u_1^2 + \frac{B_2}{2} u_2^2 \\ & + \lambda_1 \Big[\Lambda - (1-u_1)\beta S(I + \rho_1 T) - \mu S \Big] \\ & + \lambda_2 \Big[\theta(1-u_1)\beta S(I + \rho_1 T) - (\mu + \delta)E + \rho T \Big] \\ & + \lambda_3 \Big[(1-\theta)(1-u_1)\beta S(I + \rho_1 T) + \delta E - (\mu + \alpha + \gamma + u_2)I \Big] \\ & + \lambda_4 \Big[(\gamma + u_2)I - (\mu + \rho)T \Big], \end{aligned} \tag{6.4}$$

where $\lambda_i(t)$, $i = 1, \ldots, 4$, are the adjoint variables associated with the state variables S, E, I, T, respectively.

Proposition 6.1. *There exists an optimal control pair $(u_1^*, u_2^*) \in \mathcal{U}$ with corresponding state trajectories that minimize J. Furthermore, there exists adjoint*

functions $\lambda_1, \cdots, \lambda_4$ *such that*

$$\begin{cases} {}^{C}D_t^q\lambda_1 = \lambda_1\Big((1-u_1)\beta(I+\rho_1 T)+\mu\Big) - \lambda_2\,\theta(1-u_1)\beta(I+\rho_1 T) \\ \qquad\qquad - \lambda_3(1-\theta)(1-u_1)\beta(I+\rho_1 T), \\ {}^{C}D_t^q\lambda_2 = (\mu+\delta)\lambda_2 - \delta\lambda_3, \\ {}^{C}D_t^q\lambda_3 = -K_1 + \lambda_1(1-u_1)\beta S - \lambda_2\theta(1-u_1)\beta S \\ \qquad\qquad - \lambda_3\Big((1-\theta)(1-u_1)\beta S - (\mu+\alpha+\gamma+u_2)\Big) - \lambda_4(\gamma+u_2), \\ {}^{C}D_t^q\lambda_4 = -K_2 + \lambda_1(1-u_1)\beta\rho_1 S - \lambda_2\Big(\theta(1-u_1)\beta\rho_1 S + \rho\Big) \\ \qquad\qquad - \lambda_3(1-\theta)(1-u_1)\beta\rho_1 S + (\mu+\rho)\lambda_4, \end{cases} \tag{6.5}$$

together with the transversality conditions

$$\lambda_1(t_f) = \lambda_2(t_f) = \lambda_3(t_f) = \lambda_4(t_f) = 0. \tag{6.6}$$

Moreover, the optimal controls are characterized by

$$\begin{aligned} u_1^*(t) &= \min\left\{1, \max\left\{0, \frac{\beta S(t)(I(t)+\rho_1 T(t))\big(\lambda_2(t)\theta + \lambda_3(t)(1-\theta) - \lambda_1(t)\big)}{B_1}\right\}\right\}, \\ u_2^*(t) &= \min\left\{1, \max\left\{0, \frac{I(t)(\lambda_3(t)-\lambda_4(t))}{B_2}\right\}\right\}. \end{aligned} \tag{6.7}$$

Proof. From Corollary 4.1 of Fleming and Rishel (see [10]), the convexity of the integrand in the cost functional J ensures the existence of at least one optimal control pair (u_1^*, u_2^*) minimizing J. In addition, the application of the generalized Pontryagin's maximum principle leads to the adjoint system and the transversality conditions stated.

Applying Pontryagin's Maximum Principle to the fractional control system (6.1) yields the adjoint system

$${}^{C}D_t^q\lambda_i = -\frac{\partial \mathcal{H}}{\partial x_i}, \qquad x_i \in \{S, E, I, T\},$$

with terminal conditions (6.6).

Next, by using the optimality conditions

$$\frac{\partial \mathcal{H}}{\partial u_1} = 0, \qquad \frac{\partial \mathcal{H}}{\partial u_2} = 0.$$

From (6.4), we obtain

$$\frac{\partial \mathcal{H}}{\partial u_1} = B_1 u_1 + \beta S(I+\rho_1 T)\big(\lambda_1 - \lambda_2\theta - \lambda_3(1-\theta)\big),$$

and

$$\frac{\partial \mathcal{H}}{\partial u_2} = B_2 u_2 - \lambda_3 I + \lambda_4 I.$$

Hence,

$$u_1^* = \frac{\beta S(I+\rho_1 T)\big(\lambda_2\theta + \lambda_3(1-\theta) - \lambda_1\big)}{B_1}, \qquad u_2^* = \frac{I(\lambda_3 - \lambda_4)}{B_2}.$$

Since the controls are constrained to the admissible set $[0,1]$, we apply the standard projection to enforce the bounds:

$$u_i^*(t) = \min\left\{1, \max\left\{0, u_i^*(t)\right\}\right\}, \qquad \text{for } i = 1, 2.$$

Therefore, the explicit expressions of the optimal controls are given by:

$$\begin{aligned} u_1^*(t) &= \min\left\{1, \max\left\{0, \frac{\beta S(t)(I(t)+\rho_1 T(t))\big(\lambda_2(t)\theta + \lambda_3(t)(1-\theta) - \lambda_1(t)\big)}{B_1}\right\}\right\}, \\ u_2^*(t) &= \min\left\{1, \max\left\{0, \frac{I(t)(\lambda_3(t) - \lambda_4(t))}{B_2}\right\}\right\}. \end{aligned} \tag{6.8}$$

This completes the proof. □

7. Numerical simulations

In this section, we present the simulation results of the fractional-order model using MATLAB Software.

7.1. **Simulations on the stability of equilibrium points.** The numerical simulations are carried out using the following parameter values in order to analyze the dynamics of the population for different values of the fractional order q. The initial conditions used for the numerical simulations are given by $(S_0, E_0, I_0, T_0) = (800,\ 400,\ 250,\ 150)$.

In Fig. 3, we observe that for different values of the fractional order q, when $\mathcal{R}_0 < 1$, the curves corresponding to the infected population converge to zero as time increases. This indicates the progressive elimination of the disease from the population. At the same time, the susceptible and treated populations tend toward constant values, confirming that the system approaches the disease-free equilibrium and stabilizes in the absence of infection.

Fig. 4 illustrates the global asymptotic stability of the endemic equilibrium when $\mathcal{R}_0 > 1$. It can be observed that both infected and non-infected populations converge toward positive steady-state values corresponding to the endemic equilibrium for various values of the fractional order q. This behavior confirms that when $\mathcal{R}_0 > 1$, the disease persists permanently within the population.

Several values of the fractional order, namely $q = 0.60$, $q = 0.75$, and $q = 1$, were considered to investigate their influence on the model dynamics. It was observed that for $q = 0.60$, the infected population converges more rapidly to the disease-free equilibrium, indicating a faster eradication of the disease compared to larger values of q. In contrast, for $q = 0.75$ and $q = 1$, the convergence toward the disease-free equilibrium becomes slower, showing that the memory effect associated with smaller fractional orders significantly affects the speed of disease evolution.

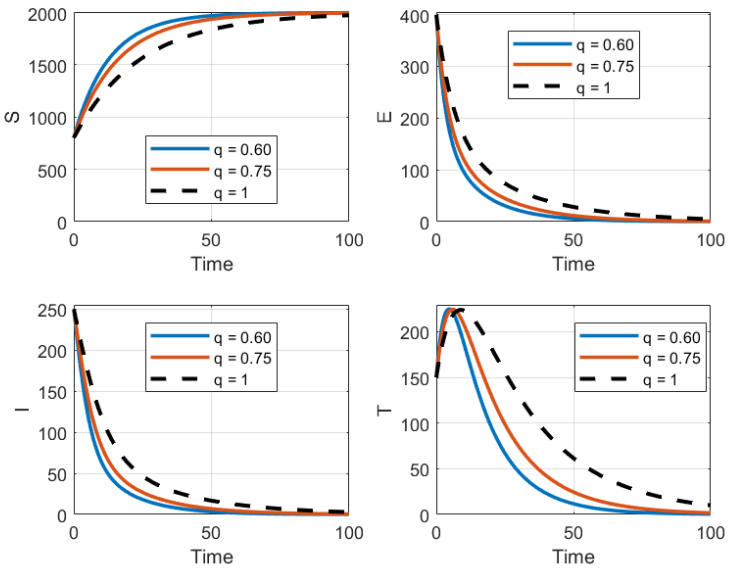


FIGURE 3. Population dynamics for $\mathcal{R}_0 = 0.400$. The parameters values used are $\Lambda = 100$, $\mu = 0.05$, $\beta = 0.00004$, $\rho_1 = 0.15$, $\theta = 0.75$, $\delta = 0.08$, $\alpha = 0.03$, $\gamma = 0.12$, $\rho = 0.02$.

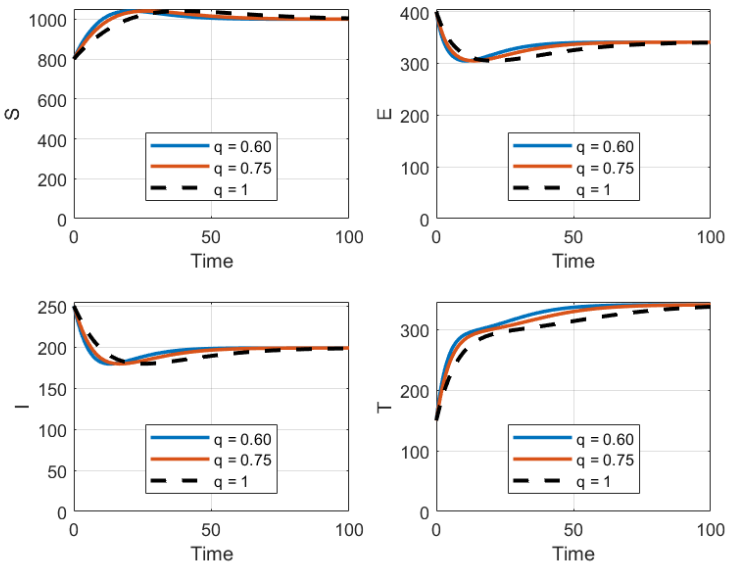


FIGURE 4. Population dynamics for $\mathcal{R}_0 = 2.000$. The parameters values used are $\Lambda = 100$, $\mu = 0.05$, $\beta = 0.0002$, $\rho_1 = 0.15$, $\theta = 0.75$, $\delta = 0.08$, $\alpha = 0.03$, $\gamma = 0.12$, $\rho = 0.02$.

7.2. **Comparison of the Integer and Fractional Model.** The dynamics of the system without intervention clearly show that when $\mathcal{R}_0 < 1$ (case illustrated

in Fig. 3), the disease is progressively eliminated in both cases, integer ($q = 1$) and fractional ($q < 1$). However, it is noteworthy that the rate of convergence toward the disease-free equilibrium is faster for lower fractional orders (for example, $q = 0.60$ vs. $q = 1$). This result highlights the ability of the fractional model to capture memory effects and to reflect real epidemiological dynamics with greater temporal accuracy.
In contrast, when $\mathcal{R}_0 > 1$ (Fig. 4), the model predicts the persistence of the disease with a stable endemic equilibrium. Again, although the qualitative behavior is similar between the integer and fractional models, the temporal trajectory shows significant differences depending on q, suggesting that the fractional model incorporates delayed phenomena that are not captured within an integer-order framework.

7.3. **Optimal control simulation.** To numerically solve the fractional optimal control problem, we use the Forward-Backward Sweep Method (FBSM) (see [16]). This iterative procedure consists of integrating the state system forward in time and the adjoint system backward in time, while successively updating the control variables until convergence.
Fig. 5 presents the dynamics of the infected population under the implementation of the prevention strategy u_1 only. It is observed that the application of u_1 significantly reduces the number of infected individuals compared to the uncontrolled case.

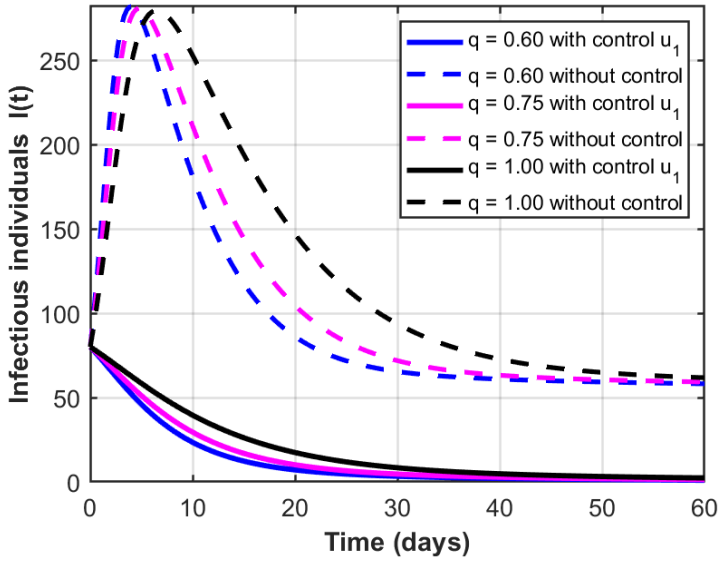


FIGURE 5. Dynamics of infected individuals with and without the optimal control u_1

Fig. 6 shows the effect of the treatment control u_2 alone. In this case, a more pronounced reduction in the infected population is observed. The reinforcement of treatment accelerates the removal of infectious individuals, leading to a faster decline in infection levels.

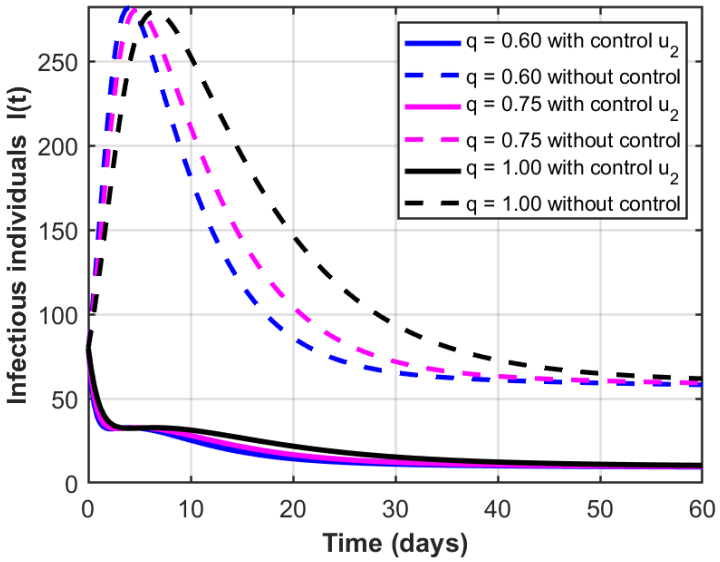


FIGURE 6. Dynamics of infected individuals with and without the optimal control u_2

Fig. 7 illustrates the combined effect of both controls u_1 and u_2. The simultaneous implementation of prevention and treatment strategies leads to a drastic reduction in the infected population, driving the system toward disease elimination. In the absence of control measures, the infected population initially increases and then gradually decreases toward a positive endemic level, indicating the long-term persistence of tuberculosis within the community.
This result confirms the strong synergistic effect of the two control measures and demonstrates that their combination is the most effective strategy to control the tuberculosis transmission.

8. Conclusion

In this paper, we have proposed and analyzed a fractional-order tuberculosis model incorporating prevention and treatment strategies. The use of fractional calculus provides a more realistic framework for describing tuberculosis transmission by accounting for memory effects and hereditary properties, which are essential characteristics of chronic infectious diseases with latency and possible reactivation.
The basic reproduction number $\mathcal{R}_0$ was derived using the next-generation matrix approach and used as a threshold parameter for determining disease persistence. We established the existence, positivity, and boundedness of solutions to guarantee the biological relevance of the model. The global stability analyses of both the disease-free equilibrium and the endemic equilibrium were rigorously investigated. By constructing appropriate Lyapunov functions, sufficient conditions ensuring the global asymptotic stability of the equilibria were obtained. In particular, the disease-free equilibrium is globally and asymptotically stable when

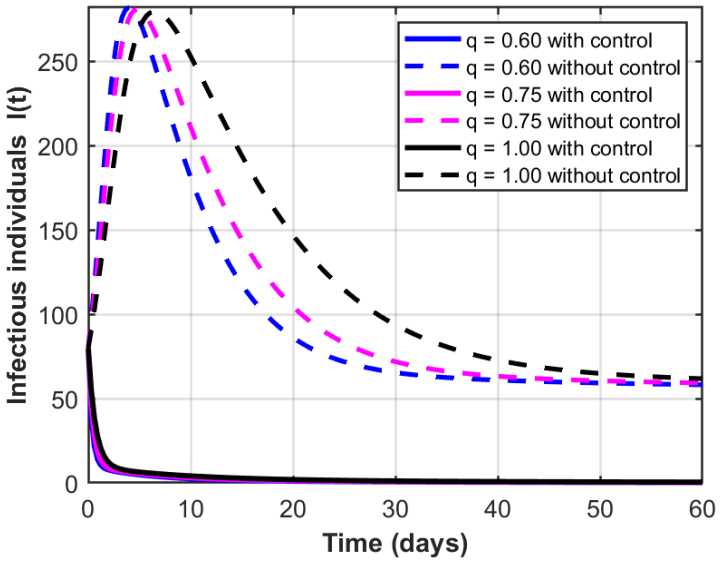


FIGURE 7. Dynamics of infected individuals with and without the optimal controls u_1 and u_2.

$\mathcal{R}_0 < 1$, indicating disease elimination, whereas the endemic equilibrium persists when $\mathcal{R}_0 > 1$.

A sensitivity analysis of $\mathcal{R}_0$ was carried out to identify the parameters that most strongly influence tuberculosis transmission. The results showed that the transmission coefficient β, the recruitment rate Λ, the treatment rate γ, and the infectious contribution of treated individuals represented by ρ_1 play major roles in the spread of the disease. These findings provide useful guidance for prioritizing effective intervention strategies and improving public health decision-making.

Furthermore, an optimal control problem was formulated by introducing two time-dependent control variables: the prevention effort $u_1(t)$, which reduces the effective transmission rate, and the treatment effort $u_2(t)$, which improves the recovery rate of infectious individuals. Using Pontryagin's Maximum Principle, the necessary conditions for optimality were derived and numerically solved. The simulation results showed that the combined implementation of prevention and treatment is significantly more effective than applying a single strategy, leading to a substantial reduction in the number of infectious individuals and the overall disease burden while maintaining reasonable implementation costs.

Overall, this study confirms that fractional-order epidemic modeling combined with optimal control theory provides a powerful mathematical framework for understanding and managing tuberculosis dynamics. It highlights the importance of integrating prevention campaigns and treatment reinforcement in order to achieve efficient disease control and possible eradication.

For future research, it would be interesting to extend this work by considering more general fractional operators such as the Caputo–Fabrizio and Atangana–Baleanu derivatives, as well as incorporating time delays, reinfection mechanisms, and stochastic perturbations to better reflect real epidemiological conditions.

Acknowledgement. Acknowledgements could be placed at the end of the text but precede the references.

References

1. Apelblat, A. (2020). Differentiation of the Mittag-Leffler functions with respect to parameters in the Laplace transform approach. *Mathematics*, 8(5), 657. https://doi.org/10.3390/math8050657
2. Balzotti, C., D'Ovidio, M., Lai, A. C., & Loreti, P. (2021). Effects of fractional derivatives with different orders in SIS epidemic models. *Computation*, 9(8), 89. https://doi.org/10.3390/computation9080089
3. Bhatter, S., Kumawat, S., Purohit, S. D., & Suthar, D. L. (2025). Mathematical modeling of tuberculosis using Caputo fractional derivative: A comparative analysis with real data. *Scientific Reports*, 15(1), 12672. https://doi.org/10.1038/s41598-025-97502-5
4. Chagdal, M., Aarir, M., Harroudi, S., & Allali, K. (2026). Stability of a fractional multi-strain epidemic model. *Gulf Journal of Mathematics*, 24(1). https://doi.org/10.56947/ce7vg982
5. Daimary, N., & Paul, R. (2024). Analysis of a fractional-order mathematical model for occupational transition from farming to other sectors. *Gulf Journal of Mathematics*, 18(1), 165–188. https://doi.org/10.56947/gjom.v18i1.2196
6. Dicko, H., Traoré, A., & Ouedraogo, D. (2024). Dynamics of a SVEIR epidemic model with a delay in diagnosis in a changing environment. *Contemporary Mathematics*, 5, 3762–3789. https://doi.org/10.37256/cm.5320244865
7. Dicko, H., & Traoré, A. (2025). Analysis of tuberculosis model with the impact of hospital resources. *Journal of Applied Mathematics and Computing*, 71, 3305–3328. https://doi.org/10.1007/s12190-024-02356-1
8. Dicko, H., Traoré, A., & Ouedraogo, R. (2025). Analysis and optimal control of a fractional tuberculosis model. *Applications of Mathematics*, 70(5), 671–694. https://doi.org/10.21136/AM.2025.0075-25
9. Diethelm, K. (2010). *The analysis of fractional differential equations: An application-oriented exposition using differential operators of Caputo type*. Lecture Notes in Mathematics, 2004. Springer Berlin Heidelberg. https://doi.org/10.1007/978-3-642-14574-2
10. Fleming, W. H., & Rishel, R. W. (1975). *Deterministic and stochastic optimal control*. Stochastic Modelling and Applied Probability, 1. Springer-Verlag. https://doi.org/10.1007/978-1-4612-6380-7
11. Hardy, G. H., Littlewood, J. E., & Pólya, G. (1952). *Inequalities* (2nd ed.). Cambridge University Press.
12. Khan, A., Shah, K., Abdeljawad, T., & Amacha, I. (2024). Fractal fractional model for tuberculosis: Existence and numerical solutions. *Scientific Reports*, 14(1), 12211. https://doi.org/10.1038/s41598-024-62386-4
13. Hamdan, N. I., & Kilicman, A. (2018). A fractional order SIR epidemic model for dengue transmission. *Chaos, Solitons & Fractals*, 114, 55–62. https://doi.org/10.1016/j.chaos.2018.06.031
14. Kumar, R. P., Santra, P. K., & Mahapatra, G. S. (2023). Global stability and analysing the sensitivity of parameters of a multiple-susceptible population model of SARS-CoV-2 emphasising vaccination drive. *Mathematics and Computers in Simulation*, 203, 741–766. https://doi.org/10.1016/j.matcom.2022.07.012
15. La Salle, J. P. (1976). *The stability of dynamical systems*. Society for Industrial and Applied Mathematics. https://doi.org/10.1137/1.9781611970432
16. Lenhart, S., & Workman, J. T. (2007). *Optimal control applied to biological models*. Chapman & Hall/CRC.

17. Li, Y., Liu, X., Yuan, Y., Li, J., & Wang, L. (2022). Global analysis of tuberculosis dynamical model and optimal control strategies based on case data in the United States. *Applied Mathematics and Computation*, 422, 126983. https://doi.org/10.1016/j.amc.2022.126983
18. Rangkuti, Y. M., Firmansyah, & Landong, A. (2022). Sensitivity analysis of SEIR epidemic model of Covid 19 spread in Indonesia. *Journal of Physics: Conference Series*, 2193(1), 012092. https://doi.org/10.1088/1742-6596/2193/1/012092
19. Sheng, H., Li, Y., & Chen, Y. (2011). Application of numerical inverse Laplace transform algorithms in fractional calculus. *Journal of the Franklin Institute*, 348(2), 315–330. https://doi.org/10.1016/j.jfranklin.2010.11.009
20. Tilahun, G. T., Wolle, G. A., & Tofik, M. (2021). Eco-epidemiological model and analysis of potato leaf roll virus using fractional differential equation. *Arab Journal of Basic and Applied Sciences*, 28(1), 41–50. https://doi.org/10.1080/25765299.2020.1865621
21. Traoré, A., Ouedraogo, R., & Dicko, H. (2026). Analysis and optimal control of a fractional-order model of a vector-borne disease. *International Journal of Dynamics and Control*, 14(5), 152. https://doi.org/10.1007/s40435-026-02092-3
22. Van den Driessche, P., & Watmough, J. (2002). Reproduction numbers and sub-threshold endemic equilibria for compartmental models of disease transmission. *Mathematical Biosciences*, 180(1–2), 29–48. https://doi.org/10.1016/S0025-5564(02)00108-6
23. World Health Organization. (2023). *Global tuberculosis report 2023*. World Health Organization. https://www.who.int/publications/i/item/9789240083851
24. Yang, Y., Tang, S., Ren, X., Zhao, H., & Guo, C. (2016). Global stability and optimal control for a tuberculosis model with vaccination and treatment. *Discrete and Continuous Dynamical Systems - Series B*, 21(3), 1009–1022. https://doi.org/10.3934/dcdsb.2016.21.1009
25. Zhang, J., Li, Y., & Zhang, X. (2015). Mathematical modeling of tuberculosis data of China. *Journal of Theoretical Biology*, 365, 159–163. https://doi.org/10.1016/j.jtbi.2014.10.019

[1] Laboratoire de Mathématiques et Informatique, Université Joseph KI-ZERBO, 03 BP 7021 Ouagadougou 03, Burkina Faso.
Email address: desiweder@yahoo.fr

[2] Laboratoire de Mathématiques, Informatique et Applications, Université Norbert ZONGO, BP 376 Koudougou, Burkina Faso.
Email address: dickoh507@gmail.com

[3] Laboratoire d'Analyse Numérique, d'Informatique et de Biomathématiques, Université Joseph KI-ZERBO, 03 BP 7021 Ouagadougou 03, Burkina Faso.
Email address: kiemtoreadama@gmail.com